

Supersymmetric Interpretation of the Muon $g - 2$ Anomaly

Motoi Endo,^(a,b,c) Koichi Hamaguchi,^(c,d) Sho Iwamoto,^(e) and Teppei Kitahara^(f,g)

^(a) *KEK Theory Center, IPNS, KEK, Tsukuba, Ibaraki 305-0801, Japan*

^(b) *The Graduate University of Advanced Studies (Sokendai), Tsukuba, Ibaraki 305-0801, Japan*

^(c) *Kavli IPMU (WPI), UTIAS, The University of Tokyo, Kashiwa, Chiba 277-8583, Japan*

^(d) *Department of Physics, The University of Tokyo, Bunkyo-ku, Tokyo 113-0033, Japan*

^(e) *ELTE Eötvös Loránd University, Pázmány Péter sétány 1/A, Budapest H-1117, Hungary*

^(f) *Institute for Advanced Research, Nagoya University, Nagoya 464-8601, Japan*

^(g) *Kobayashi-Maskawa Institute for the Origin of Particles and the Universe,
Nagoya University, Nagoya 464-8602, Japan*

Abstract

The Fermilab Muon $g - 2$ collaboration recently announced the first result of measurement of the muon anomalous magnetic moment ($g - 2$), which confirmed the previous result at the Brookhaven National Laboratory and thus the discrepancy with its Standard Model prediction. We revisit low-scale supersymmetric models that are naturally capable to solve the muon $g - 2$ anomaly, focusing on two distinct scenarios: chargino-contribution dominated and pure-bino-contribution dominated scenarios. It is shown that the slepton pair-production searches have excluded broad parameter spaces for both two scenarios, but they are not closed yet. For the chargino-dominated scenario, the models with $m_{\tilde{\mu}_L} \gtrsim m_{\tilde{\chi}_1^\pm}$ are still widely allowed. For the bino-dominated scenario, we find that, although slightly non-trivial, the region with low $\tan \beta$ with heavy higgsinos is preferred. In the case of universal slepton masses, the low mass regions with $m_{\tilde{\mu}} \lesssim 230 \text{ GeV}$ can explain the $g - 2$ anomaly while satisfying the LHC constraints. Furthermore, we checked that the stau-bino coannihilation works properly to realize the bino thermal relic dark matter. We also investigate heavy staus case for the bino-dominated scenario, where the parameter region that can explain the muon $g - 2$ anomaly is stretched to $m_{\tilde{\mu}} \lesssim 1.3 \text{ TeV}$.

KEYWORDS: Muon $g - 2$, Supersymmetry phenomenology

Contents

1	Introduction	1
2	Chargino contributions	3
2.1	Setup and Result	4
2.2	LHC constraints	6
3	Bino contributions	8
3.1	Setup	8
3.2	Constraints	9
3.3	Result in universal slepton mass case	11
3.4	Result in heavy stau case	15
4	Conclusions and Discussion	17

1 Introduction

The success of the Standard Model (SM) has been confirmed by the Higgs boson discovery, the Higgs coupling measurements, recent results from the Large Hadron Collider (LHC), and a number of low-energy precision measurements in the quark and lepton flavor physics. However, physics beyond the SM (BSM) is definitely required, for example, in order to explain the dark matter.

The muon anomalous magnetic moment [the muon $g - 2$; $a_\mu \equiv (g_\mu - 2)/2$] may be a hint to construct BSM scenarios, for there has laid 3.7σ -level discrepancy between its SM prediction [1],^{#1}

$$a_\mu^{\text{SM}} = (11\,659\,181.0 \pm 4.3) \times 10^{-10}, \quad (1)$$

and the value measured at the Brookhaven National Laboratory in 1997–2001 [11–13],^{#2}

$$a_\mu^{\text{BNL}} = (11\,659\,208.9 \pm 5.4_{\text{stat}} \pm 3.3_{\text{sys}}) \times 10^{-10}. \quad (2)$$

The effort on experimental reconfirmation of this anomaly has been made by the Fermilab Muon $g - 2$ collaboration [15] and the J-PARC muon $g - 2$ /EDM collaboration

^{#1}Recent development of the lattice calculation including QED and isospin-breaking corrections [2] has revealed that the leading-order hadronic vacuum polarization contributions disagree with those calculated by the data-driven approach at 2.3σ level [1, 3–6] and the resultant Δa_μ is zero-consistent within 2σ level. In order to explain the 2.3σ discrepancy while saving the global fit of the electroweak sector, the cross section $\sigma(e^+e^- \rightarrow \text{hadrons})$ below 1 GeV region has to be changed [7–9]. A dedicated study for such the energy region is given in Ref. [10].

^{#2}This value is calculated with the latest value of the muon-to-proton magnetic ratio [1, 14].

[16, 17]. These on-going experiments aim to reduce the experimental error at least by a factor of four compared to a_μ^{BNL} . Very recently, the Fermilab Muon $g - 2$ collaboration presented the first result on the measurement [18, 19],

$$a_\mu^{\text{FNAL}; 2021\text{Apr.}} = (11\,659\,204.0 \pm 5.4) \times 10^{-10}, \quad (3)$$

corresponding to 3.3σ level. Together with the BNL measurement, the average value of the a_μ measurements is given by [18, 19]

$$a_\mu^{\text{BNL+FNAL}} = (11\,659\,206.1 \pm 4.1) \times 10^{-10}. \quad (4)$$

Now the discrepancy between the experimental and theoretical values amounts to

$$\Delta a_\mu \equiv a_\mu^{\text{BNL+FNAL}} - a_\mu^{\text{SM}} = (25.1 \pm 5.9) \times 10^{-10}, \quad (5)$$

whose significance is equivalent to 4.2σ level, and the muon $g - 2$ anomaly is reconfirmed.^{#3}

This discrepancy is as large as the SM electroweak contribution to the muon $g - 2$, $a_\mu(\text{EW}) = (15.4 \pm 0.1) \times 10^{-10}$ [1], which implies that BSM physics around the electroweak scale may be responsible for it. Low-energy supersymmetry (SUSY) is one of such solutions. Its contribution to the muon $g - 2$, which we denote by a_μ^{SUSY} , can naturally explain the discrepancy because it is amplified by model-specific parameters as we shall see [21–23]. One can also benefit from the merits of SUSY models, such as the explanation of the gauge hierarchy problem, the gauge coupling unification, and the existence of the dark matter candidate as the lightest SUSY particle (LSP); this makes SUSY more attractive.

The SUSY contributions to the muon $g - 2$ can be sizable when at least *three* SUSY multiplets are as light as $\mathcal{O}(100)$ GeV. They are classified into four types: “WHL”, “BHL”, “BHR”, and “BLR”, where W, B, H, L, and R stand for wino, bino, higgsino, left-handed and right-handed smuons, respectively. Under the mass-insertion approximation, these four types are given as [23]^{#4}

$$a_\mu^{\text{WHL}} = \frac{\alpha_2}{4\pi} \frac{m_\mu^2}{M_{2\mu}} \tan\beta \cdot f_C \left(\frac{M_2^2}{m_{\tilde{\nu}_\mu}^2}, \frac{\mu^2}{m_{\tilde{\nu}_\mu}^2} \right) - \frac{\alpha_2}{8\pi} \frac{m_\mu^2}{M_{2\mu}} \tan\beta \cdot f_N \left(\frac{M_2^2}{m_{\tilde{\mu}_L}^2}, \frac{\mu^2}{m_{\tilde{\mu}_L}^2} \right), \quad (6)$$

$$a_\mu^{\text{BHL}} = \frac{\alpha_Y}{8\pi} \frac{m_\mu^2}{M_{1\mu}} \tan\beta \cdot f_N \left(\frac{M_1^2}{m_{\tilde{\mu}_L}^2}, \frac{\mu^2}{m_{\tilde{\mu}_L}^2} \right), \quad (7)$$

$$a_\mu^{\text{BHR}} = -\frac{\alpha_Y}{4\pi} \frac{m_\mu^2}{M_{1\mu}} \tan\beta \cdot f_N \left(\frac{M_1^2}{m_{\tilde{\mu}_R}^2}, \frac{\mu^2}{m_{\tilde{\mu}_R}^2} \right), \quad (8)$$

$$a_\mu^{\text{BLR}} = \frac{\alpha_Y}{4\pi} \frac{m_\mu^2 M_{1\mu}}{m_{\tilde{\mu}_L}^2 m_{\tilde{\mu}_R}^2} \tan\beta \cdot f_N \left(\frac{m_{\tilde{\mu}_L}^2}{M_1^2}, \frac{m_{\tilde{\mu}_R}^2}{M_1^2} \right), \quad (9)$$

^{#3}Very recently, the hadronic light-by-light contribution was analyzed in the first principle by the lattice QCD calculation [20]. The significance of the anomaly could decrease slightly.

^{#4}Note that the exact analytic formulae are used in our analysis instead of relying on this approximation. See discussion below.

where M_1 (M_2) is the bino (wino) soft mass, μ is the higgsino mass parameter, $\tan\beta = v_u/v_d$ is the ratio of the vacuum expectation values of the up- and down-type Higgs, and $m_{\tilde{\mu}_{L/R}}$ and $m_{\tilde{\nu}_\mu}$ are the masses of the left/right-handed smuon and the muon sneutrino, respectively. The loop functions are given by

$$f_C(x, y) = xy \left[\frac{5 - 3(x+y) + xy}{(x-1)^2(y-1)^2} - \frac{2 \ln x}{(x-y)(x-1)^3} + \frac{2 \ln y}{(x-y)(y-1)^3} \right], \quad (10)$$

$$f_N(x, y) = xy \left[\frac{-3 + x + y + xy}{(x-1)^2(y-1)^2} + \frac{2x \ln x}{(x-y)(x-1)^3} - \frac{2y \ln y}{(x-y)(y-1)^3} \right], \quad (11)$$

which satisfy $0 \leq f_{C/N}(x, y) \leq 1$, $f_C(1, 1) = 1/2$ and $f_N(1, 1) = 1/6$. An important fact is that the first three contributions, a_μ^{WHL} , a_μ^{BHL} , and a_μ^{BHR} , are enhanced by $\tan\beta$ but suppressed as μ increases. On the other hand, the last one, a_μ^{BLR} , is enhanced by $\mu \tan\beta$. This difference provides us with two completely distinct scenarios.

In this paper, we revisit two branches of the SUSY scenarios proposed to explain the muon $g-2$ anomaly:^{#5} one in which the chargino contribution, a_μ^{WHL} , is dominant, and the other in which the pure-bino contribution, a_μ^{BLR} , is dominant.^{#6} This work focuses on the minimal setups, where only three or four SUSY multiplets are light to have sizable a_μ^{WHL} or a_μ^{BLR} , while the other irrelevant particles are decoupled. Although this approach lacks specific SUSY-breaking models and does not cover the whole possible Minimal Supersymmetric Standard Model (MSSM) models, it allows us to clarify the relevant MSSM parameters and tell which LHC (and other) constraints are relevant, compared to studies with scans over the whole parameter space.^{#7}

This paper is organized as follows. In Sec. 2, we revisit the parameter regions in which $a_\mu^{\text{SUSY}} \approx a_\mu^{\text{WHL}}$, based on our previous study [48]. Compared with Ref. [48], the new a_μ measurements [19], the new theory combination [1], and new results from the LHC [49, 50] are implemented. In Sec. 3, we revisit the bino-contribution to the muon $g-2$, a_μ^{BLR} , taking into account of the latest LHC constraints as well as the vacuum meta-stability. A related analysis was performed in our previous study [51]. Interestingly, a wider region of the parameter space is allowed for smaller $\tan\beta$, rather than the large $\tan\beta$ case. We study the cases with and without flavor universal slepton masses. We also discuss an implication for the dark matter abundance with the bino-slepton coannihilation. Section 4 is devoted to conclusions and discussion.

2 Chargino contributions

In this section, we consider the parameter regions where the chargino contribution to the muon $g-2$ is dominant, based on our previous study [48].

^{#5}For recent studies of the muon $g-2$ motivated SUSY models based on the LHC Run 2 results, see, *e.g.*, Refs. [24–47].

^{#6}The other contributions, a_μ^{BHL} and a_μ^{BHR} , can also be dominant. See, *e.g.*, Ref. [27].

^{#7}This strategy has been taken in, *e.g.*, the following works: Refs. [28, 29, 48] with particular focus on WHL, Refs. [27, 41] on BHL and BHR, and Refs. [41, 45, 47] considering the combination of the contributions.

2.1 Setup and Result

The setup in this section is as follows:

- Among SUSY particles, neutralinos $\tilde{\chi}_i^0$, charginos $\tilde{\chi}_j^\pm$, and left-handed sleptons $\tilde{l}_L, \tilde{\nu}$ are within the LHC reach, *i.e.*, with masses of $\lesssim 1$ TeV. Here, \tilde{l} denotes $\tilde{e}, \tilde{\mu}$, and $\tilde{\tau}$.
- The right-handed sleptons \tilde{l}_R are heavy, so that a_μ^{BHR} and a_μ^{BLR} are suppressed and our analysis is simplified. The scalar trilinear terms $(A_e)_{ij}$ are neglected for simplicity.
- The soft masses of the left-handed sleptons are flavor universal and diagonal.
- All the colored SUSY particles (gluino and squarks) are decoupled. This assumption makes the LHC constraints more conservative, while their contribution to the muon $g - 2$ is negligibly small even if they are light because it arises at the two-loop level. In addition, heavy colored SUSY particles are motivated by the mass of the SM-like Higgs boson as well as by LHC constraints.
- The heavy Higgs bosons, whose contributions to a_μ^{SUSY} are also negligible, are decoupled as well.

Then, the following five model parameters are left relevant:

$$M_1, \quad M_2, \quad \mu, \quad m_L^2, \quad \tan \beta, \quad (12)$$

where m_L stands for the universal soft mass for the left-handed sleptons, and as in Ref. [48], the following four subspace of the parameters are analyzed:^{#8}

$$(A) \quad M_1 = \frac{1}{2}M_2, \quad \mu = M_2, \quad \tan \beta = 40, \quad (13)$$

$$(B) \quad M_1 = \frac{1}{2}M_2, \quad \mu = 2M_2, \quad \tan \beta = 40, \quad (14)$$

$$(C) \quad m_{\tilde{\chi}_1^0} = 100 \text{ GeV}, \quad \mu = M_2, \quad \tan \beta = 40, \quad (15)$$

$$(D) \quad m_{\tilde{\chi}_1^0} = 100 \text{ GeV}, \quad \mu = 2M_2, \quad \tan \beta = 40. \quad (16)$$

The analyses is done in the same manner as in Ref. [48]. In particular, SDECAY 1.5a [53,54] and GM2Calc 1.5.0 [55] are utilized to calculate the decay rates and a_μ^{SUSY} , respectively, and the right-handed slepton mass parameter m_R is taken to be $m_R = 3$ TeV.

The results are shown in Fig. 1 under the axes being the physical masses of the lighter chargino $\tilde{\chi}_1^\pm$ and the left-handed smuon $\tilde{\mu}_L$. The SUSY contribution to the muon $g - 2$ is shown by the black solid contours in terms of $a_\mu^{\text{SUSY}} \times 10^{10}$. The parameter spaces where a_μ^{SUSY} solves the discrepancy $\Delta a_\mu = (25.1 \pm 5.9) \times 10^{-10}$ at the 1σ (2σ) level are shown by the orange-filled (yellow-filled) regions. The LHC Run 2 constraints are shown

^{#8}We here require that the LSP is the bino-like neutralino with ignorance of the dark matter overabundance. The relic density may be reduced to be consistent with the observed one by an entropy production or considering more generic parameter space of the SUSY models (cf. [47]). Meanwhile, Ref. [52] focuses on a similar scenario in which a_μ^{WHL} explains the anomaly with $M_1 > M_2, \mu$, *i.e.*, a wino-higgsino mixed neutralino as the LSP.

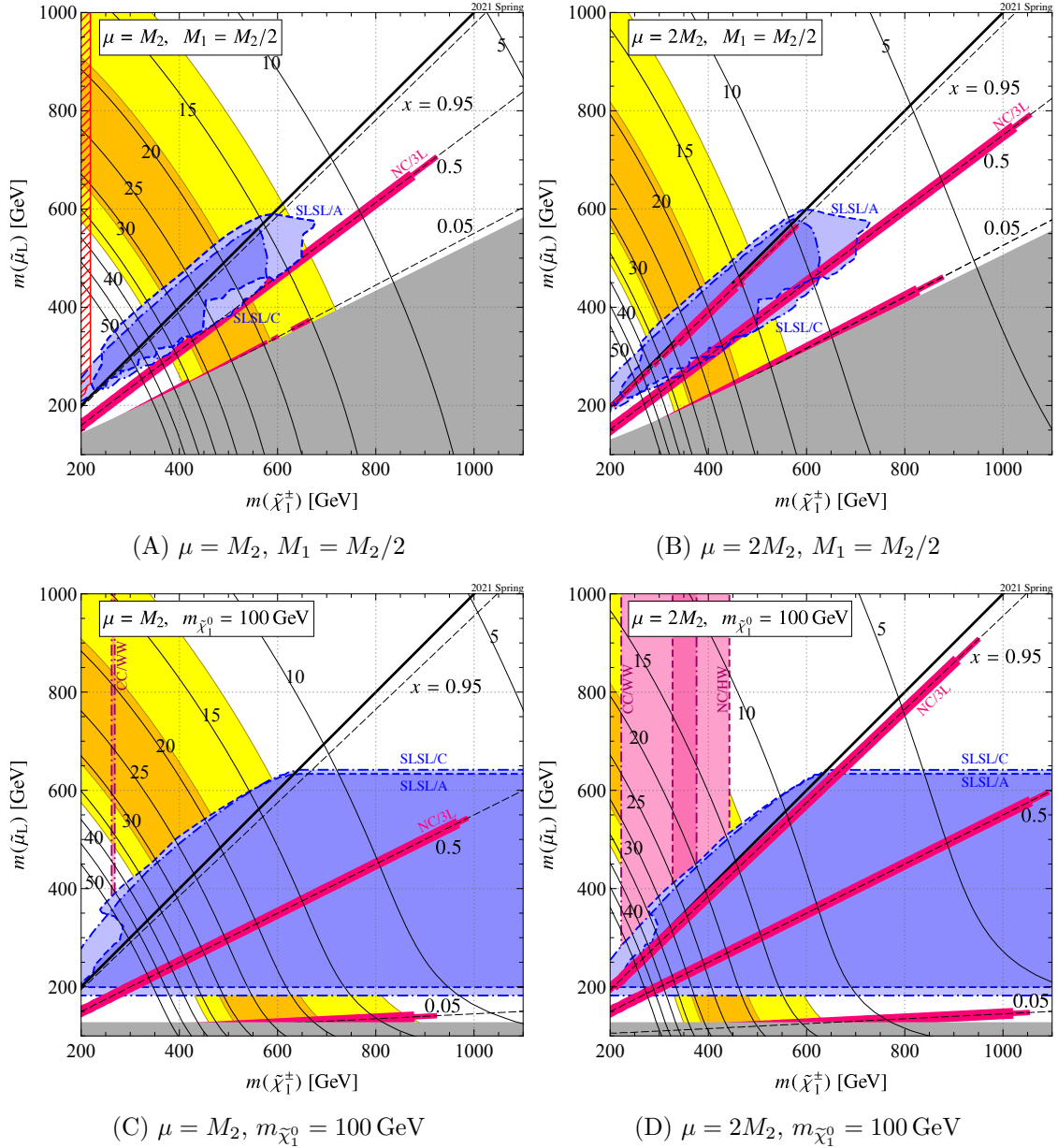


Figure 1: The 2021 Spring summary of the chargino-dominated SUSY scenario for the muon $g - 2$ anomaly. Four benchmark parameter planes are considered, where the WHL contribution is sizable and a_μ^{SUSY} explains the anomaly at the 1σ (2σ) level in the orange-filled (yellow-filled) regions; $a_\mu^{\text{SUSY}} \times 10^{10}$ is shown by the black contours (but up to 50). The thick black line corresponds to $m_{\tilde{\mu}_L} = m_{\tilde{\chi}_1^\pm}$. The gray-filled region, where the LSP is $\tilde{\nu}$, and the red-hatched region in (A), which corresponds to a compressed spectrum, are not studied. The red-filled and blue-filled regions are excluded by the LHC experiment [50, 56, 57]. We also analyzed the results of Refs. [58, 59] but only on the model points with $x = 0.05, 0.5$, and 0.95 [see Eq. (22)]; the excluded ranges are shown by the magenta bars. Detailed description of the LHC constraints is provided in our previous work [48].

Table 1: Benchmark points for the chargino-contribution dominated scenario. The mass parameters are in units of GeV.

	WHL1	WHL2	WHL3
M_1	200	200	102
M_2	400	400	400
μ	400	800	400
m_L	600	600	600
$\tan\beta$	40	40	40
$m_{\tilde{\mu}_1}, m_{\tilde{\tau}_1}$	602	602	602
$m_{\tilde{\nu}_{\mu,\tau}}$	597	597	597
$m_{\tilde{\chi}_1^0}$	196	199	100
$m_{\tilde{\chi}_2^0}$	347	394	346
$m_{\tilde{\chi}_3^0}$	405	803	406
$m_{\tilde{\chi}_4^0}$	462	810	461
$m_{\tilde{\chi}_1^\pm}$	346	394	346
$m_{\tilde{\chi}_2^\pm}$	462	811	462
$a_\mu^{\text{SUSY}} \times 10^{10}$	24	15	24

by blue-filled regions, red-filled regions, and magenta lines at the 95% confidence level; they are described in the next subsection.

We find that, as far as considering the parameter space in Fig. 1, models with $m_{\tilde{\mu}_L} < m_{\tilde{\chi}_1^\pm}$ are strongly disfavored as a solution to the muon $g - 2$ anomaly. Meanwhile, for models with $m_{\tilde{\mu}_L} > m_{\tilde{\chi}_1^\pm}$, LHC constraints are not critical yet; those models may explain the muon $g - 2$ anomaly and are to be searched for at the future LHC runs. In Table 1, we show the mass spectra and the SUSY contribution to the muon $g - 2$ (a_μ^{SUSY}) for some viable benchmark points in Fig. 3. The production cross sections and the branching fractions of the SUSY particles for those points can be found in Ref. [48].

2.2 LHC constraints

In the present setup, direct pair productions of neutralinos, charginos, and sleptons are the targets at LHC searches. We consider the following channels which have been studied

by the ATLAS and CMS collaborations:

$$\text{SLSL: } pp \rightarrow \tilde{\ell}_L \tilde{\ell}_L^* \rightarrow (\ell \tilde{\chi}_1^0)(\bar{\ell} \tilde{\chi}_1^0), \quad (17)$$

$$\text{CC/WW: } pp \rightarrow \tilde{\chi}_1^+ \tilde{\chi}_1^- \rightarrow (W^+ \tilde{\chi}_1^0)(W^- \tilde{\chi}_1^0), \quad (18)$$

$$\text{NC/HW: } pp \rightarrow \tilde{\chi}_2^0 \tilde{\chi}_1^\pm \rightarrow (h \tilde{\chi}_1^0)(W^\pm \tilde{\chi}_1^0), \quad (19)$$

$$\text{NC/ZW: } pp \rightarrow \tilde{\chi}_2^0 \tilde{\chi}_1^\pm \rightarrow (Z \tilde{\chi}_1^0)(W^\pm \tilde{\chi}_1^0), \quad (20)$$

$$\text{NC/3L: } pp \rightarrow \tilde{\chi}_2^0 \tilde{\chi}_1^\pm \rightarrow \begin{cases} (\tilde{l}_L)(\nu \tilde{l}_L) \rightarrow (l \tilde{\chi}_1^0)(\nu l \tilde{\chi}_1^0), \\ (\tilde{l}_L)(\tilde{l}\tilde{\nu}) \rightarrow (l \tilde{\chi}_1^0)(l\nu \tilde{\chi}_1^0). \end{cases} \quad (21)$$

where $\ell = e, \mu$, $\tilde{\ell}_L = \tilde{e}_L, \tilde{\mu}_L$, $l = e, \mu, \tau$, $\tilde{l}_L = \tilde{e}_L, \tilde{\mu}_L, \tilde{\tau}_L$, and $\tilde{\nu} = \tilde{\nu}_{e,L}, \tilde{\nu}_{\mu,L}, \tilde{\nu}_{\tau,L}$. For the details of the analysis procedure, we refer the readers to our previous study [48].

In the previous work [48], the parameter spaces were constrained by the following analyses:

- Ref. [56] by ATLAS collaboration (SLSL, 139 fb^{-1}),
- Ref. [57] by ATLAS collaboration (CC/WW and NC/HW, 139 fb^{-1}),
- Ref. [58] by CMS collaboration (NC/3L, 35.9 fb^{-1}),
- Ref. [59] by ATLAS collaboration (NC/3L, 36.1 fb^{-1}).

In addition, we found that the newly appeared result,^{#9}

- Ref. [50] by CMS collaboration (SLSL, 139 fb^{-1})

is also responsible for the exclusion of our parameter spaces; it excludes the blue-filled region with labels ‘‘SLSL/C’’ in Fig. 1. The ‘‘SLSL/A’’ blue-filled region has been excluded by the ATLAS counterpart. The red-filled regions are excluded by the CC/WW and NC/HW channels. For the NC/3L channel, both of the ATLAS and CMS collaborations assume specific mass spectra of electroweakinos and sleptons, which determine the lepton energies. In terms of a mass difference ratio,

$$x = \frac{m_{\tilde{\mu}_L} - m_{\tilde{\chi}_1^0}}{m_{\tilde{\chi}_1^\pm} - m_{\tilde{\chi}_1^0}}, \quad (22)$$

the CMS collaboration considers three different mass spectra, $x = (0.05, 0.5, 0.95)$, while the ATLAS studies $x = 0.5$. In Fig. 1, the corresponding model points are displayed by the dashed black lines, and the magenta bars show the regions excluded by the NC/3L channel. Although we have not investigated the NC/3L bounds for arbitrary x value, it is expected that the bounds on $x = 0.05, 0.5, 0.95$ are continuously connected with a peak around $x = 0.5$ (cf. Ref. [60]).

Several preliminary results on conference papers [61–63] are not included because numerical data have not been made public. According to our estimation, they provide

^{#9}We also examined the NC/HW analysis in Ref. [49] and the NC/ZW analysis in Ref. [50] based on the full Run 2 data, but no constraints are obtained on our parameter space. Other fifteen publications from the ATLAS and CMS collaborations are also taken into account; see [48] for the full list of references.

additional constraints based on the NC/3L and NC/HW signatures. The new NC/3L result [62] will confirm that our parameter spaces with $m_{\tilde{\mu}_L} < m_{\tilde{\chi}_1^\pm}$ are strongly disfavored, while the new NC/HW result [63] will exclude more region with $m_{\tilde{\mu}_L} > m_{\tilde{\chi}_1^\pm}$, where the impact depends on the LSP mass.

3 Bino contributions

In the previous section, the wino was assumed to be light to enhance the chargino contributions to the muon $g - 2$. However, such an assumption is not always necessary for the SUSY contributions to be sizable. In this section, we consider another scenario in which the neutralino contribution is dominant. In particular, as shown in Eq. (9), the bino contribution a_μ^{BLR} becomes large when $\mu \tan \beta$ is large and the bino-like neutralino, the left- and right-handed sleptons are light.

3.1 Setup

Let us summarize our setup in this section.

- The bino-like neutralino $\tilde{\chi}_1^0$, left-handed sleptons $\tilde{l}_L, \tilde{\nu}$ and right-handed sleptons \tilde{l}_R are assumed to be light. In addition, the higgsinos may be relatively light when $\tan \beta$ is large.
- The wino is assumed to be decoupled. Then, the chargino contributions a_μ^{WHL} discussed in Sec. 2 are suppressed even when μ is relatively small.
- As in the previous section, all the colored SUSY particles and the heavy Higgs bosons are decoupled.
- We assume the scalar trilinear terms $(A_e)_{ij}$ to be zero for simplicity.^{#10}

Then, the following five model parameters are left relevant:

$$M_1, \quad \mu, \quad (m_L^2)_i, \quad (m_R^2)_i, \quad \tan \beta, \quad (23)$$

where m_L and m_R represent the soft masses for the left- and right-handed sleptons, respectively, with the flavor index $i = \tilde{e}, \tilde{\mu}, \tilde{\tau}$. More concretely, we consider the following two subspace of the parameters:

- Universal slepton mass: $(m_L)_{\tilde{e}} = (m_L)_{\tilde{\mu}} = (m_L)_{\tilde{\tau}}$ and $(m_R)_{\tilde{e}} = (m_R)_{\tilde{\mu}} = (m_R)_{\tilde{\tau}}$.
- Heavy stau: $(m_L)_{\tilde{\tau}} > (m_L)_{\tilde{e}}$ and $(m_R)_{\tilde{\tau}} > (m_R)_{\tilde{e}}$.

Although a_μ^{BLR} is independent of the stau mass, some of the constraints discussed below depend on it. It will be shown that much wider parameter space is allowed for the heavy stau scenario.

In addition to the one-loop contribution a_μ^{BLR} , there are non-negligible two-loop corrections. Among them, QED corrections [64] and those to the Yukawa couplings [65, 66] are

^{#10}The Bino contribution a_μ^{BLR} can be enhanced by extremely large $(A_e)_{22}$ instead of enlarging μ and $\tan \beta$.

taken into account in this section. The latter corrections are also included in calculating the slepton mass spectra and mixing matrices. In order to treat them consistently when the corrections are large, we do not use `GM2Calc` in the following analysis. Meanwhile, we neglect radiative corrections to the neutralino couplings, which are not decoupled by heavy SUSY particles (see Refs. [51, 67–72]). Although the Bino coupling is equal to the gauge coupling at the tree level, this equality is violated by the SUSY-breaking effects, and the deviations are enlarged when the soft SUSY-breaking scale is large. According to the renormalization group approach [51], they can amount to 5–10% corrections to a_μ^{SUSY} when the soft masses, especially the wino mass, are as large as 10–100 TeV. Other higher-order contributions are not-yet-estimated or expected to be smaller.

3.2 Constraints

When the bino and sleptons are light, there are several phenomena which are potentially correlated with the muon $g - 2$. We consider the following four constraints:

- LHC (and LEP) searches for the SUSY particles,
- Higgs coupling measurements,
- neutralino LSP as a candidate of the dark matter,
- stability of the electroweak vacuum.

Let us discuss them in turn. First, similarly to the previous section, the LHC experiment has studied signatures of the direct slepton productions,

$$pp \rightarrow \tilde{\ell}\tilde{\ell}^* \rightarrow (\ell\tilde{\chi}_1^0)(\bar{\ell}\tilde{\chi}_1^0). \quad (24)$$

From this SLSL channel, where events with energetic two electrons or muons are studied, lower bounds on the lightest neutralino mass are obtained as a function of the slepton mass by the ATLAS collaboration (8 TeV, 20.3 fb⁻¹) [73], (13 TeV, 139 fb⁻¹) [56], and the CMS collaboration (13 TeV, 139 fb⁻¹) [50]. Furthermore, the ATLAS collaboration has studied the compressed mass spectrum of the neutralino and sleptons. From the SLSL-soft channel, where events with low-transverse momentum electrons or muons are studied, bounds on the slepton masses are obtained for the mass difference $\lesssim 30$ GeV (13 TeV, 139 fb⁻¹) [74]. Furthermore, we impose the LEP bound on the stau mass, $m_{\tilde{\tau}_1} > 95.7$ GeV [75].

In addition, events with two energetic hadronically-decaying taus have been studied to search for the direct stau pair productions. Although we investigated the latest results by the ATLAS collaboration (13 TeV, 139 fb⁻¹) [76] and the CMS collaboration (13 TeV, 77.2 fb⁻¹) [77], their constraints were found to be weaker than the above. Also, the smuon/selectron masses are limited by the LEP results [75, 78]. The constraints are weaker than 100 GeV and out of the range of our plots.

The decays of the SM-like Higgs boson have been measured well at the LHC experiment. Among the various decay channels, the staus may affect the branching ratio of $h \rightarrow \gamma\gamma$ especially when $\mu \tan \beta$ is large and the staus are light [79–82].^{#11} Currently, the

^{#11}Effects of smuons or selectrons are much weaker because the Yukawa couplings are tiny.

signal strength^{#12} has been measured to be [83]

$$\mu_{\gamma\gamma}|_{\text{PDG average}} = \frac{\Gamma(h \rightarrow \gamma\gamma)}{\Gamma(h \rightarrow \gamma\gamma)_{\text{SM}}} = 1.11^{+0.10}_{-0.09}, \quad (25)$$

which is consistent with the SM prediction ($\mu_{\gamma\gamma}^{\text{SM}} = 1$).^{#13} Meanwhile, the measurement is expected to be improved in future; the precision may reach $\delta\mu_{\gamma\gamma}/\mu_{\gamma\gamma} = 3\text{--}4\%$ at HL-LHC (14 TeV, 6 ab^{-1}) or ILC (1 TeV, 8 ab^{-1}), 2% if they are combined, and would be 0.6% at FCC-ee/eh/hh [84].

In the analysis, we require that the lightest neutralino is the LSP.^{#14} Although it is one of the best-known candidates of the dark matter, if it is almost composed of the bino, its thermal relic abundance easily exceeds the measured value [83, 85],

$$\Omega_{\text{DM}}h^2 = 0.1200 \pm 0.0012. \quad (26)$$

In the present setup, the neutralino relic abundance can be consistent with this result by the slepton coannihilation, *i.e.*, when the slepton mass is close to the lightest neutralino appropriately. We estimate the relic abundance of the LSP neutralino by using the public package `micrOMEGAs 5.2.7.a` [86–89].

Such a dark matter may be detected by the direct detection. The LUX [90], PandaX-II [91] and XENON1T [92] experiments have provided stringent constraints on the spin-independent cross section of the dark matter scattering off the nuclei. In the analysis, the cross section is estimated by using `micrOMEGAs`.

The last constraint is the vacuum meta-stability condition. The trilinear coupling of the sleptons and the SM-like Higgs boson is given by

$$V \simeq -\frac{m_\ell}{\sqrt{2}v(1 + \Delta_\ell)} \mu \tan \beta \cdot \tilde{\ell}_L^* \tilde{\ell}_R h + \text{h.c.}, \quad (27)$$

where $v \simeq 174 \text{ GeV}$ is the vacuum expectation value of the SM-like Higgs, and Δ_ℓ represents the radiative corrections to the lepton Yukawa couplings mentioned above [66]. As $\mu \tan \beta$ increases, the trilinear coupling is enhanced, charge-breaking minima become deeper, and eventually, the stability of the electroweak vacuum is spoiled. We require the lifetime of the vacuum being longer than the age of the Universe, restricting $|\mu \tan \beta|$ from

^{#12}To be exact, the production cross section and the total width of the Higgs boson may also be modified by the SUSY particles. However, the staus barely affect it, and we ignore such contributions.

^{#13}The CMS collaboration recently reported a preliminary result, $\mu_{\gamma\gamma} = 1.12 \pm 0.09$, using the LHC Run 2 full data. Although it has not been accounted in the above PDG average, the result is consistent with Eq. (25), and the following results are almost unchanged.

^{#14}The lightest charged slepton is likely to be lighter than sneutrinos when $\mu \tan \beta$ is large enough.

above. For the following analysis, we adopt the fitting formula explored in Refs. [51, 93],

$$\begin{aligned} & \left| \frac{m_\ell \mu \tan \beta}{\sqrt{2}v(1 + \Delta_\ell)} \right| \\ & \leq \eta_\ell \left\{ 1.01 \times 10^2 \text{ GeV} \sqrt{(m_L)_{\tilde{\ell}}(m_R)_{\tilde{\ell}}} + 1.01 \times 10^2 \text{ GeV} [(m_L)_{\tilde{\ell}} + 1.03(m_R)_{\tilde{\ell}}] \right. \\ & \quad \left. + \frac{2.97 \times 10^6 \text{ GeV}^3}{(m_L)_{\tilde{\ell}} + (m_R)_{\tilde{\ell}}} - 1.14 \times 10^8 \text{ GeV}^4 \left[\frac{1}{(m_L^2)_{\tilde{\ell}}} + \frac{0.983}{(m_R^2)_{\tilde{\ell}}} \right] - 2.27 \times 10^4 \text{ GeV}^2 \right\}, \end{aligned} \quad (28)$$

with $\ell = e, \mu, \tau$. The numerical evaluation was done by the bounce method [94] via `CosmoTransitions 1.0.2` [95].^{#15} A factor $\eta_\ell \sim 1$ provides a mild $\tan \beta$ dependence coming from the Yukawa contributions to the quartic terms in the scalar potential. The explicit value of η_ℓ is found in Refs. [51, 93].

3.3 Result in universal slepton mass case

Let us first consider the slepton universal mass case. The left-handed (also right-handed) selectron, smuon and stau have a common soft SUSY-breaking mass,

$$(m_L)_{\tilde{e}} = (m_L)_{\tilde{\mu}} = (m_L)_{\tilde{\tau}}, \quad (m_R)_{\tilde{e}} = (m_R)_{\tilde{\mu}} = (m_R)_{\tilde{\tau}}. \quad (29)$$

Such a spectrum is motivated to avoid dangerous lepton flavor or CP violations (see Ref. [51]). The SUSY contribution to the muon $g - 2$ cannot be arbitrarily large because $\mu \tan \beta$ is bounded from above; due to the stau left-right mixing, a too large $\mu \tan \beta$ can violate one (or more) of the following constraints, (i) the vacuum stability in the stau-Higgs potential, Eq. (28), (ii) the neutralino being the LSP, *i.e.*, $m_{\tilde{\tau}_1} > m_{\tilde{\chi}_1^0}$, and (iii) the LEP bound on the stau mass, $m_{\tilde{\tau}_1} > 95.7 \text{ GeV}$. Thus, these conditions yield an upper bound on the μ parameter as a function of M_1 , $(m_L)_{\tilde{\tau}}$, and $(m_R)_{\tilde{\tau}}$.

Figure 2 shows the results for $m_L = m_R$ and $\tan \beta = 5, 10, 30, 50$. The horizontal and vertical axes are the physical masses of the lightest neutralino $\tilde{\chi}_1^0$ and the lighter smuon $\tilde{\mu}_1$, respectively. For a given set of $m_L (= m_R)$, M_1 , and $\tan \beta$, the μ parameter (or equivalently $\mu \tan \beta$) is maximized under the above conditions, so that a_μ^{BLR} becomes maximum. In the orange-filled (yellow-filled) regions, the SUSY contribution explains the muon $g - 2$ discrepancy at the 1σ (2σ) level. Below the black line in each figure, a_μ^{SUSY} exceeds the central value of Δa_μ [Eq. (5)] for the maximized μ parameter. In other words, in these regions, a_μ^{SUSY} can be optimized by reducing the μ parameter. The upper edges of these muon $g - 2$ regions, *i.e.*, the upper bounds on $m_{\tilde{\chi}_1^0}$, are determined by the condition $m_{\tilde{\tau}_1} > m_{\tilde{\chi}_1^0}$.^{#16} In the low mass region of $m_{\tilde{\chi}_1^0} \lesssim 100 \text{ GeV}$, the LEP bound on the stau mass also affects the boundary. Meanwhile, without the LHC constraints, there would be

^{#15}Note that we ignore thermal effects and radiative corrections to the formula, which may affect the following result [96, 97] and will be discussed elsewhere.

^{#16}To be exact, $\tilde{\tau}_1$ becomes long-lived if $m_{\tilde{\tau}_1}$ is too much close to $m_{\tilde{\chi}_1^0}$. Thus, $m_{\tilde{\tau}_1} - m_{\tilde{\chi}_1^0} \gtrsim 2 \text{ GeV}$ is required in practice, though the figures are almost unchanged.

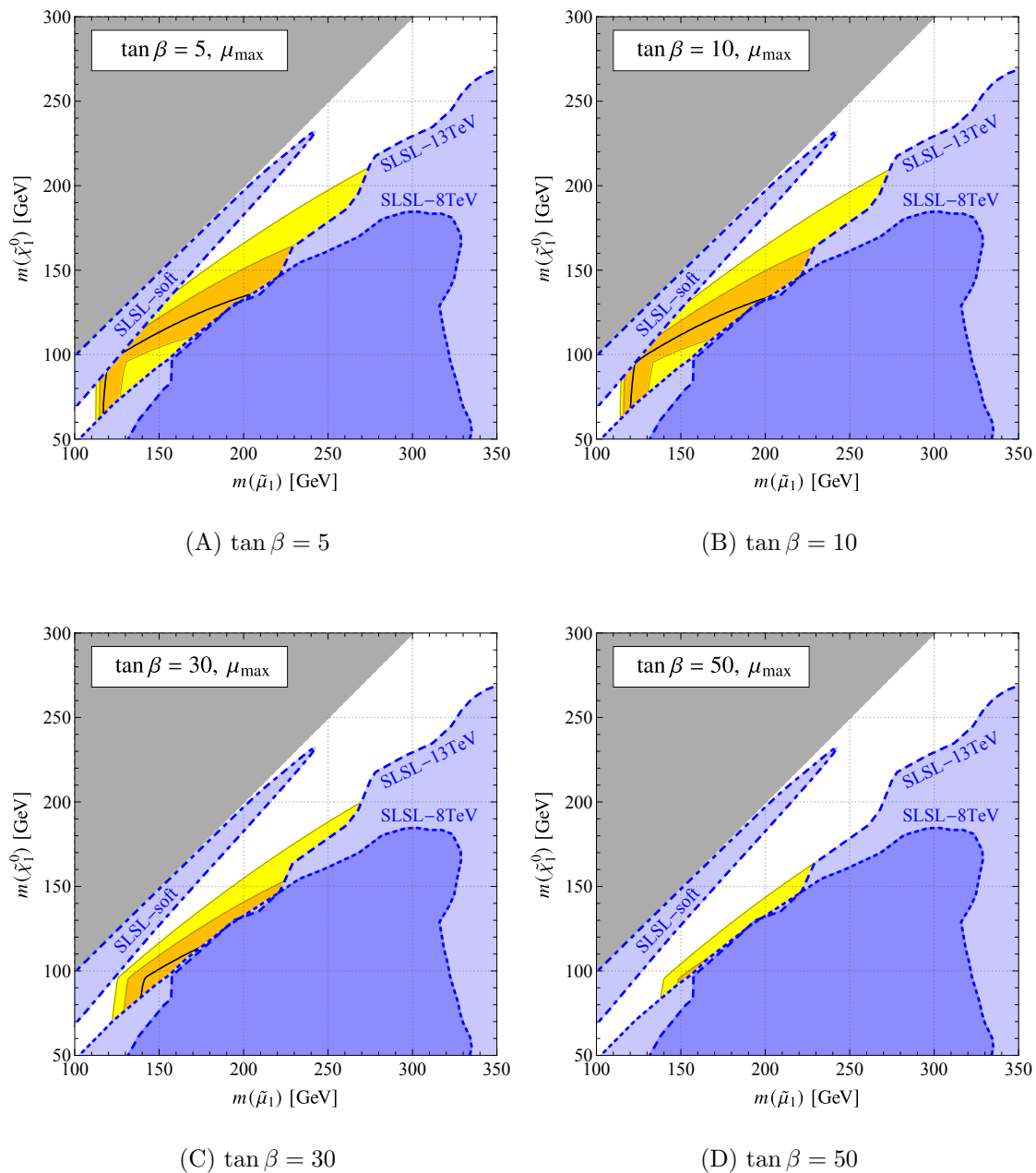


Figure 2: The summary of the bino-dominated SUSY scenario for the muon $g-2$ anomaly. The universal slepton mass with $m_L = m_R$ is assumed. Four planes respectively correspond to $\tan \beta = 5, 10, 30$ and 50 . The μ parameter is maximized (μ_{\max}) at each point under the conditions described in the text. The muon $g-2$ anomaly can be explained at the 1σ (2σ) level in the orange-filled (yellow-filled) regions. Below the black line in each figure, a_μ^{SUSY} exceeds the central value of Δa_μ in Eq. (5) for the maximized μ parameter. In the gray-filled regions, $\tilde{\mu}_1$ is lighter than $\tilde{\chi}_1^0$. The blue-filled regions are excluded by the LHC slepton searches [50, 56, 73, 74].

lower boundaries (*i.e.*, lower bounds on $m_{\tilde{\chi}_1^0}$, or equivalently upper bounds on $m_{\tilde{\mu}_1}$) due to the vacuum meta-stability condition, though they are hidden by the LHC constraints from the SLSL channel (lower blue-filled regions). Here, the region with smaller $m_{\tilde{\mu}_1}$ is constrained by the ATLAS 8 TeV result, while the larger one is by the ATLAS 13 TeV result. Besides, the SLSL-soft channel restricts the regions of degenerate neutralino-smuon masses (upper blue-filled region).

In Fig. 2 (A), (B), which correspond to $\tan\beta = 5, 10$ respectively, $\tilde{\mu}_1$ is required to be $m_{\tilde{\mu}_1} \lesssim 230$ (270) GeV to explain the muon $g - 2$ discrepancy at the 1σ (2σ) level. It is noticed that the regions become narrower as $\tan\beta$ increases (see Fig. 2 (C), (D) for $\tan\beta = 30, 50$). The reason is as follows. At each set of $(M_1, m_L = m_R)$, the upper bound on $\mu \tan\beta$ is almost unchanged. Then, since larger $\tan\beta$ leads to smaller μ , the BHR contribution to a_μ^{SUSY} , which destructively interferes with a_μ^{BLR} , becomes enhanced when μ is smaller, *i.e.*, $\tan\beta$ is large. Note that the BHL contribution is weaker than that of BHR for $m_L \sim m_R$ [see Eqs. (7) and (8)]. Consequently, lower $\tan\beta$ is favored to enhance a_μ^{SUSY} . Note that $\mu \sim 500$ GeV–4 TeV for $\tan\beta = 10$ in the muon $g - 2$ region of Fig. 2 (A), which are large enough to suppress a_μ^{BHL} and a_μ^{BHR} .

The branching ratio of $h \rightarrow \gamma\gamma$ is affected by light staus with large $\mu \tan\beta$. The signal strength is likely to be enhanced in the vicinity of the boundary of the SLSL constraint, while it is weaker for larger $m_{\tilde{\chi}_1^0}$ as the upper bound on $\mu \tan\beta$ is tighter.^{#17} Around the muon $g - 2$ regions in the figures, it can be deviated from the SM value $\mu_{\gamma\gamma}$ by 2–5% at most, which satisfies the current limit (25) and is accessible in future by HL-LHC, ILC, or FCC-ee/eh/hh.

In Fig. 2, the thermal relic abundance of $\tilde{\chi}_1^0$ is not tuned to reproduce the dark matter value (26). After imposing the LHC constraints, we found that the abundances in the muon $g - 2$ region satisfy $\Omega_{\tilde{\chi}_1^0} < \Omega_{\text{DM}}$ because the stau masses are well close to that of $\tilde{\chi}_1^0$. Let us next consider the case where $\mu \tan\beta$ is determined by requiring that the thermal relic abundance of the neutralino is equal to Eq. (26). It is almost determined by the coannihilations with the lightest stau.^{#18} In Fig. 3, the muon $g - 2$ discrepancy is explained at the 1σ (2σ) level in the orange-filled (yellow-filled) regions while satisfying $\Omega_{\tilde{\chi}_1^0} h^2 = 0.12$. Here, $\tan\beta = 5$ (A) and 10 (B) with $m_L = m_R$. It is found that $\tilde{\mu}_1$ is required to be $m_{\tilde{\mu}_1} \lesssim 220$ (270) GeV to explain the muon $g - 2$ discrepancy at the 1σ (2σ) level.

In the figures, the left boundaries of the orange-filled (yellow-filled) regions for small $m_{\tilde{\chi}_1^0}$ are determined by the XENON1T constraint of the dark matter direct detection [92]. Here, μ cannot be so large, and thus, the dark matter-nucleon elastic scattering cross-section is enhanced. For smaller $\tan\beta$, wider parameter regions are allowed because the coannihilation works efficiently by larger μ , *i.e.*, without the well-tempered contributions.

^{#17}Note that contributions to $\mu_{\gamma\gamma}$ coming from light chargino loops may amount to additional few % at most. Such contributions, however, are scaled by $\approx 1/(\mu M_2 \tan\beta)$ [98, 99]. Hence, they are certainly suppressed by M_2 in the present setup.

^{#18}There can be more than one values of the μ parameter that realize the desired dark matter density; in such a case, we take the largest μ as it gives the largest contribution to the muon $g - 2$.

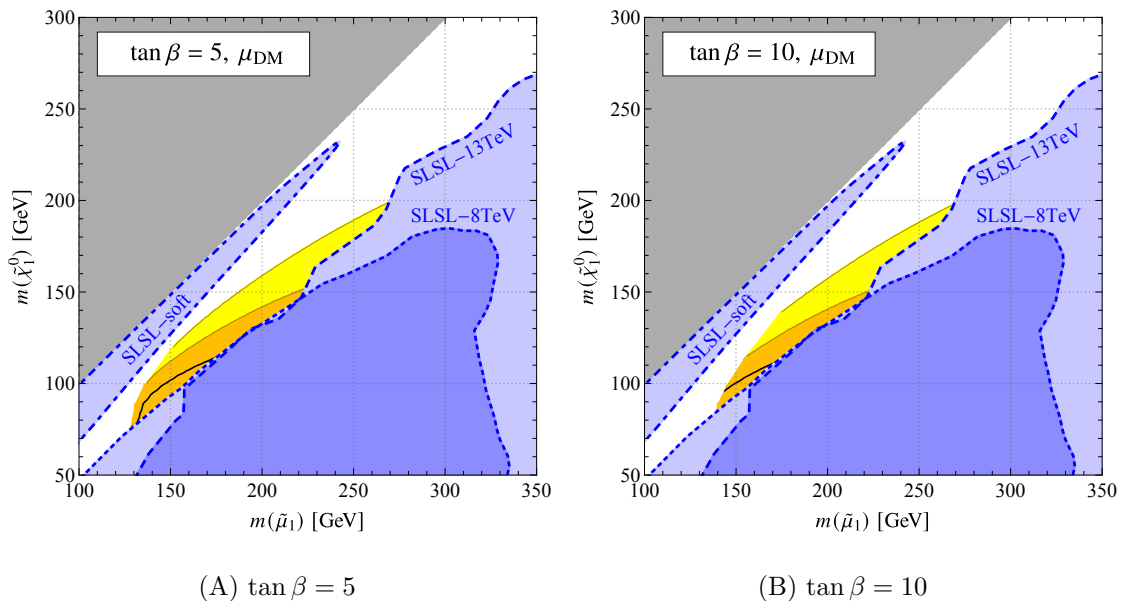


Figure 3: The bino-dominated SUSY scenario for the muon $g - 2$ anomaly with proper dark matter relic abundance. In the same way as Fig. 2, the universal slepton mass with $m_L = m_R$ are used, but the μ parameter is tuned (μ_{DM}) to realize $\Omega_{\text{DM}} h^2 = 0.12$. We show cases of $\tan \beta = 5$ and 10. In the orange-filled (yellow-filled) regions, the muon $g - 2$ anomaly can be solved at the 1σ (2σ) level while satisfying the XENON1T constraint.

In the near future, the sensitivity of the direct detection is planned to be improved by orders of magnitudes. We have checked that most of the muon $g - 2$ parameter regions can be probed by the XENONnT experiment [100] if the slepton mass spectrum is universal.

We also found that the branching ratio of the SM-like Higgs boson decay to two photons, $\mu_{\gamma\gamma}$, can deviate from the SM prediction by at most 2% in the muon $g - 2$ parameter region.

In Table 2, we show the mass spectra, the SUSY contribution to the muon $g - 2$ (a_μ^{SUSY}), the thermal relic abundance of $\tilde{\chi}_1^0$ ($\Omega_{\tilde{\chi}_1^0} h^2$), the spin-independent cross section of the neutralino for the dark matter direct detection (σ_p^{SI}), and the branching ratio of $h \rightarrow \gamma\gamma$ ($\mu_{\gamma\gamma}$) for some benchmark points in Fig. 3. The points BLR1 and BLR2 can be probed by the direct stau searches at the ILC 250 GeV, while all the four points are accessible by the ILC 500 GeV as well as the XENONnT experiment. Furthermore, all the points could be tested by measuring the branching ratio of the SM-like Higgs boson decay at FCC-ee/eh/hh.

So far, we have assumed that the soft masses of the left- and right-handed sleptons have a common value, $m_L = m_R$. According to the loop function of a_μ^{BLR} , for a fixed value of $\tilde{\mu}_1$ the SUSY contributions to the muon $g - 2$ is maximized when $m_L = m_R$, *i.e.*, the muon $g - 2$ regions in Fig. 2 [51]. Meanwhile, the stau coannihilation is realized by larger μ for $m_L \neq m_R$, which enhances a_μ^{BLR} simultaneously. Consequently, the muon $g - 2$ regions in Fig. 3 are enlarged for $m_L \neq m_R$, though we need detailed studies for the decay of the

Table 2: Benchmark points for the pure-bino-contribution dominated scenario, where the universal slepton mass is used. The mass parameters are in units of GeV.

	BLR1	BLR2	BLR3	BLR4
M_1	100	100	150	150
$m_L = m_R$	150	150	200	200
$\tan \beta$	5	10	5	10
μ	1323	678	1922	973
$m_{\tilde{\mu}_1}$	154	154	202	202
$m_{\tilde{\mu}_2}$	159	159	207	208
$m_{\tilde{\tau}_1}$	113	113	159	158
$m_{\tilde{\tau}_2}$	190	191	242	243
$m_{\tilde{\nu}_{\mu,\tau}}$	137	136	190	190
$m_{\tilde{\chi}_1^0}$	99	99	150	149
$m_{\tilde{\chi}_2^0}, m_{\tilde{\chi}_3^0}, m_{\tilde{\chi}_1^\pm}$	1323–1324	678–680	1922–1923	973–975
$a_\mu^{\text{SUSY}} \times 10^{10}$	27	27	17	17
$\Omega_{\text{DM}} h^2$	0.120	0.120	0.120	0.120
$\sigma_p^{\text{SI}} \times 10^{47} \text{ [cm}^2\text{]}$	1.7	3.7	0.8	1.9
$\mu_{\gamma\gamma}$	1.01	1.01	1.01	1.01

heavier sleptons to the lightest neutralino, which may be excluded by the SLSL search at the LHC.

3.4 Result in heavy stau case

Next, we discuss the case that the staus are heavier than selectrons and smuons,^{#19}

$$(m_L)_{\tilde{e}} = (m_L)_{\tilde{\mu}} < (m_L)_{\tilde{\tau}}, \quad (m_R)_{\tilde{e}} = (m_R)_{\tilde{\mu}} < (m_R)_{\tilde{\tau}}. \quad (30)$$

Although the stau masses are irrelevant for the SUSY contribution to the muon $g - 2$, the vacuum meta-stability condition of the stau–Higgs potential as well as the condition $m_{\tilde{\tau}_1} > m_{\tilde{\chi}_1^0}$ are relaxed as they increase. For $m_{\tilde{\tau}} \gg m_{\tilde{\ell}}$ with $\tilde{\ell} = \tilde{e}, \tilde{\mu}$, the vacuum meta-stability constraint from the smuon–Higgs potential becomes severer, and the latter condition is replaced by $m_{\tilde{\mu}_1} > m_{\tilde{\chi}_1^0}$.

^{#19}It is assumed that dangerous flavor or CP violations are suppressed by some mechanisms.

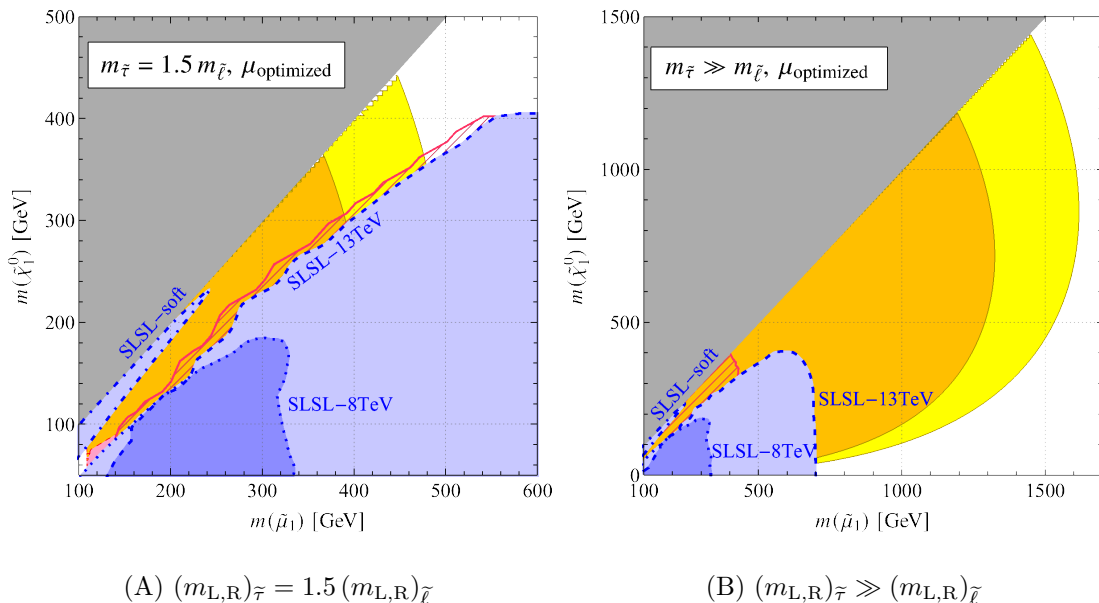


Figure 4: Same as Fig. 2, but the stau soft masses are larger than those of selectrons and smuons ($\tilde{\ell} = \tilde{e}, \tilde{\mu}$). Here, $m_L = m_R$ and $\tan\beta = 10$. The μ parameter is optimized ($\mu_{\text{optimized}}$) at each point to explain the muon $g - 2$ discrepancy at the 1σ (2σ) level in the orange-filled (yellow-filled) region. The red-hatched region is potentially excluded by the SLSL search for the decay of the heavier smuon to the lightest neutralino (see the text).

Figure 4 shows the results for (A) $(m_{L,R})_{\tilde{\tau}} = 1.5(m_{L,R})_{\tilde{\ell}}$ and (B) $(m_{L,R})_{\tilde{\tau}} \gg (m_{L,R})_{\tilde{\ell}}$. Here, each slepton satisfies $(m_L)_i = (m_R)_i$ with $\tan\beta = 10$. In the orange-filled (yellow-filled) region, the SUSY contribution can explain the muon $g - 2$ discrepancy at the 1σ (2σ) level. If $\mu \tan\beta$ is maximized under the above conditions, a_μ^{SUSY} becomes too large compared with the observed discrepancy in most of the orange-filled region. Therefore, μ is understood to be optimized at each point of these figures. The upper boundaries of the regions (the upper bound on $m_{\tilde{\chi}_1^0}$) is determined by $m_{\tilde{\mu}_1} > m_{\tilde{\chi}_1^0}$, and the right boundaries (the upper bound on $m_{\tilde{\mu}_1}$) is given by the vacuum meta-stability condition of the stau-Higgs potential in (A) and the smuon-Higgs potential in (B). As a result, it is found that $\tilde{\mu}_1$ is required to be $m_{\tilde{\mu}_1} \lesssim 390$ (490) GeV to explain the muon $g - 2$ discrepancy at the 1σ (2σ) level for $(m_{L,R})_{\tilde{\tau}} = 1.5(m_{L,R})_{\tilde{\ell}}$. As the staus become heavier, these values become larger. In the limit of $(m_{L,R})_{\tilde{\tau}} \gg (m_{L,R})_{\tilde{\ell}}$, one obtains $m_{\tilde{\mu}_1} \lesssim 1.3$ (1.6) TeV.

The blue-filled regions are excluded by the SLSL and SLSL-soft channels on the lighter smuon, and the magenta-filled region is excluded by $h \rightarrow \gamma\gamma$ [Eq. (25)] in Fig. 4 (A). In addition, the heavier smuon is potentially excluded by the SLSL search. As the staus become heavier than the smuons, $\mu \tan\beta$ is allowed to become larger, and thus, a mass splitting between the lighter and heavier smuons is enlarged especially when $m_L = m_R$. In the red-hatched region, the decay of the heavier smuon to the lightest neutralino is excluded if we suppose that $\text{BR}(\tilde{\mu}_2 \rightarrow \mu \tilde{\chi}_1^0) = 1$ and that $\mu \tan\beta$ is maximized under

the above conditions.^{#20} Although a smaller value is enough to explain the muon $g - 2$ discrepancy, detailed LHC analysis is necessary to check the viability of this region.

In Fig. 4, the relic abundance of $\tilde{\chi}_1^0$ is not tuned to reproduce the dark matter value (26), but can exceed it. In order to obtain $\Omega_{\tilde{\chi}_1^0} = \Omega_{\text{DM}}$ the smuon is required to be degenerate with the LSP appropriately for the annihilation to work. We have checked that the dark matter abundance can be reproduced for $m_{\tilde{\mu}_1} - m_{\tilde{\chi}_1^0} \lesssim 0.1 m_{\tilde{\chi}_1^0}$ while keeping the explanation to the muon $g - 2$ discrepancy, where the coannihilation works with the charged smuons, selectrons, and/or sneutrinos. We also found that the dark matter-nucleon elastic scattering cross-sections are much smaller than the XENONnT sensitivity in the heavy stau scenario.

4 Conclusions and Discussion

The first result of the measurement of the muon anomalous magnetic moment ($g - 2$) by the Fermilab Muon $g - 2$ collaboration confirmed the previous result at the Brookhaven National Laboratory and thus the long-standing discrepancy with the Standard Model prediction. In this paper, we revisited low-scale supersymmetric models as a solution to this anomaly, focusing on two distinct scenarios; one in which the chargino contribution, a_μ^{WHL} , is dominant, and the other in which the pure-bino contribution, a_μ^{BLR} , is dominant.

In the chargino-contribution dominated scenario, we revisited our previous study [48], taking account of the latest LHC results as well as the new a_μ measurements [19] and the new theory combination [1]. It was found that models with $m_{\tilde{\mu}_L} < m_{\tilde{\chi}_1^\pm}$ in this scenario are disfavored as a solution to the muon $g - 2$ anomaly, while models with $m_{\tilde{\mu}_L} > m_{\tilde{\chi}_1^\pm}$ are still widely allowed. Several benchmark points are listed in Table 1, for which a_μ^{SUSY} is sizable and the LHC constraints are still allowed.

In the pure-bino-contribution dominated scenario, we first studied the universal slepton-mass case where the μ parameter is maximized under the constraints of the vacuum stability, the neutralino being the LSP, and the LEP bound on the stau mass. Although the LHC slepton searches are tight, there remain viable parameter spaces for $m_{\tilde{\chi}_1^0} \lesssim m_{\tilde{\mu}_1} \lesssim 300$ GeV: The muon $g - 2$ anomaly can be explained within 1σ (2σ) for $m_{\tilde{\mu}_1} \lesssim 230$ (270) GeV. Interestingly, the region with low $\tan\beta$ with heavy higgsinos is preferred, because the destructive BHR contribution is suppressed.

Furthermore, the thermal relic of the bino-like neutralino can become the dominant component of the dark matter, if the stau-bino coannihilation works properly. It was shown that the relic abundance as well as the muon $g - 2$ anomaly can be explained simultaneously for $m_{\tilde{\mu}_1} \lesssim 220$ (270) GeV. Besides, such parameter regions satisfy the XENON1T constraint on the dark matter scattering cross section. We list several benchmark points in Table 2, in which the SUSY contribution to the muon $g - 2$ is sizable, the neutralino relic abundance is consistent with the measured dark matter value, and all the constraints are satisfied.

^{#20}In the universal slepton mass case, the smuon mass splitting is small enough.

We also investigated the setup that the staus are (much) heavier than the selectrons and smuons. Because the conditions of the vacuum meta-stability in the scalar potential and that the sleptons are heavier than the lightest neutralino are alleviated drastically, the parameter regions that explain the muon $g - 2$ anomaly are stretched. The muon $g - 2$ anomaly can be explained within 1σ (2σ) when $m_{\tilde{\mu}_1} \lesssim 390$ (490) GeV for $(m_{L,R})_{\tilde{\tau}} = 1.5(m_{L,R})_{\tilde{\ell}}$ and when $m_{\tilde{\mu}_1} \lesssim 1.3$ (1.6) TeV for $(m_{L,R})_{\tilde{\tau}} \gg (m_{L,R})_{\tilde{\ell}}$.

Similarly to the universal slepton mass case, the neutralino relic abundance can be consistent with that of the dark matter, if the smuon mass is within $\sim 10\%$ of the neutralino mass. We checked that the masses can become as large as ~ 1 TeV while keeping the sizable contribution to the muon $g - 2$ as well as the correct relic abundance of the dark matter. Note that the dark matter scattering cross sections are tiny and it is challenging for the dark matter direct detection.

Let us discuss future prospects in the above scenarios. For chargino-contribution dominated scenario, as mentioned in Ref. [48], future collider sensitivities may reach $m_{\tilde{\chi}_1^\pm} \lesssim 1.2\text{--}1.3$ TeV by analyzing the NC/HW channel at the HL-LHC [101, 102], and $m_{\tilde{\chi}_1^\pm} \lesssim 1.4$ (3.4) TeV at a future 100 TeV pp collider [103, 104]. Besides, the electroweakinos will be able to be probed indirectly [105–108], *e.g.*, for $m_{\tilde{\chi}_1^\pm} \lesssim 1.7\text{--}2.3$ TeV at a 100 TeV pp collider. Note that since these evaluations were performed on the simplified models, *i.e.*, the sensitivities would be degraded in realistic setups.

Meanwhile, the ILC can play essential roles in testing the pure-bino-contribution dominated scenario. In the universal slepton mass case, wide parameter regions that explain the muon $g - 2$ discrepancy are accessible by the slepton searches if the collision energy is as large as 500 GeV. The benchmark points BLR1 and BLR2 in Table 2 can be probed even at ILC 250 GeV. Furthermore, if the SUSY particles responsible for the muon $g - 2$ are within the kinematical reach, it is possible to experimentally reconstruct the SUSY contribution to the muon $g - 2$ by utilizing the precise ILC measurements [109]. It is noticed that the muon $g - 2$ parameter space falls in the region in which sleptons and the LSP are degenerate. Such spectra could also be a good target of the future LHC Runs, *e.g.*, by investigating photon collisions [110]. Furthermore, higgsinos tend to be light when the lightest neutralino is light and/or $\tan\beta$ is large. Then, their production can be probed by analyzing events with SM bosons or taus with large missing transverse momentum. Such signals will be studied elsewhere.

In the scenario where the thermal relic bino dark matter abundance is consistent with the observed one, such as the benchmark points in Table 2, most of the viable parameter space will also be probed by the XENONnT experiment. In addition, the muon $g - 2$ parameter regions can be tested by measuring the branching ratio of the SM-like Higgs boson decay at future HL-LHC, ILC and/or FCC-ee/eh/hh especially when the lightest neutralino as well as the staus are light.

The Fermilab Muon $g - 2$ collaboration has already completed Run-3 and the new results are anticipated with the full data set, which might shed further light on the SUSY scenarios.

Acknowledgments

This work is supported in part by the Grant-in-Aid for Scientific Research on Innovative Areas (No. 19H05810 [KH], No. 19H05802 [KH]), Scientific Research B (No. 16H03991 [ME], No. 20H01897 [KH]), and Early-Career Scientists (No. 16K17681 [ME] and No. 19K14706 [TK]). The work of T.K. is also supported by the JSPS Core-to-Core Program, No. JPJSCCA20200002.

References

- [1] T. Aoyama *et al.*, “The anomalous magnetic moment of the muon in the Standard Model,” *Phys. Rept.* **887** (2020) 1–166 [[arXiv:2006.04822](#)].
- [2] S. Borsanyi *et al.*, “Leading hadronic contribution to the muon 2 magnetic moment from lattice QCD,” *Nature* (2021) [[arXiv:2002.12347](#)].
- [3] G. Colangelo, M. Hoferichter, and P. Stoffer, “Two-pion contribution to hadronic vacuum polarization,” *JHEP* **02** (2019) 006 [[arXiv:1810.00007](#)].
- [4] M. Hoferichter, B.-L. Hoid, and B. Kubis, “Three-pion contribution to hadronic vacuum polarization,” *JHEP* **08** (2019) 137 [[arXiv:1907.01556](#)].
- [5] M. Davier, A. Hoecker, B. Malaescu, and Z. Zhang, “A new evaluation of the hadronic vacuum polarisation contributions to the muon anomalous magnetic moment and to $\alpha(m_Z^2)$,” *Eur. Phys. J. C* **80** (2020) 241 [[arXiv:1908.00921](#)] [*Erratum ibid.* **80** (2020) 410].
- [6] A. Keshavarzi, D. Nomura, and T. Teubner, “ $g - 2$ of charged leptons, $\alpha(M_Z^2)$, and the hyperfine splitting of muonium,” *Phys. Rev. D* **101** (2020) 014029 [[arXiv:1911.00367](#)].
- [7] A. Crivellin, M. Hoferichter, C. A. Manzari, and M. Montull, “Hadronic Vacuum Polarization: $(g - 2)_\mu$ versus Global Electroweak Fits,” *Phys. Rev. Lett.* **125** (2020) 091801 [[arXiv:2003.04886](#)].
- [8] A. Keshavarzi, W. J. Marciano, M. Passera, and A. Sirlin, “Muon $g - 2$ and $\Delta\alpha$ connection,” *Phys. Rev. D* **102** (2020) 033002 [[arXiv:2006.12666](#)].
- [9] B. Malaescu and M. Schott, “Impact of correlations between a_μ and α_{QED} on the EW fit,” *Eur. Phys. J. C* **81** (2021) 46 [[arXiv:2008.08107](#)].
- [10] G. Colangelo, M. Hoferichter, and P. Stoffer, “Constraints on the two-pion contribution to hadronic vacuum polarization,” *Phys. Lett. B* **814** (2021) 136073 [[arXiv:2010.07943](#)].
- [11] **Muon g-2** Collaboration, “Measurement of the positive muon anomalous magnetic moment to 0.7 ppm,” *Phys. Rev. Lett.* **89** (2002) 101804 [[hep-ex/0208001](#)].
- [12] **Muon g-2** Collaboration, “Measurement of the negative muon anomalous magnetic moment to 0.7 ppm,” *Phys. Rev. Lett.* **92** (2004) 161802 [[hep-ex/0401008](#)].

- [13] **Muon g-2** Collaboration, “Final Report of the Muon E821 Anomalous Magnetic Moment Measurement at BNL,” *Phys. Rev.* **D73** (2006) 072003 [[hep-ex/0602035](#)].
- [14] E. Tiesinga, P. J. Mohr, D. B. Newell, and B. N. Taylor, “The 2018 CODATA Recommended Values of the Fundamental Physical Constants.” <http://physics.nist.gov/constants> (Web Version 8.0), 2019.
- [15] **Muon g-2** Collaboration, “Muon $g - 2$ Technical Design Report.” [arXiv:1501.06858](#).
- [16] **J-PARC g-2** Collaboration, “Measurement of muon $g - 2$ and EDM with an ultra-cold muon beam at J-PARC,” *Nucl. Phys. Proc. Suppl.* **218** (2011) 242–246.
- [17] M. Abe *et al.*, “A New Approach for Measuring the Muon Anomalous Magnetic Moment and Electric Dipole Moment,” *PTEP* **2019** (2019) 053C02 [[arXiv:1901.03047](#)].
- [18] C. Polly, on behalf of **Muon g-2** Collaboration, “First results from the Muon g-2 experiment at Fermilab,” 7 Apr. 2021. Seminar talk given at Fermilab.
- [19] **Muon g-2** Collaboration, “Measurement of the Positive Muon Anomalous Magnetic Moment to 0.46 ppm,” *Phys. Rev. Lett.* **126** (2021) 141801 [[arXiv:2104.03281](#)].
- [20] E.-H. Chao, *et al.*, “Hadronic light-by-light contribution to $(g - 2)_\mu$ from lattice QCD: a complete calculation.” [arXiv:2104.02632](#).
- [21] J. L. Lopez, D. V. Nanopoulos, and X. Wang, “Large $(g - 2)_\mu$ in $SU(5) \times U(1)$ Supergravity Models,” *Phys. Rev.* **D49** (1994) 366–372 [[hep-ph/9308336](#)].
- [22] U. Chattopadhyay and P. Nath, “Probing Supergravity Grand Unification in the Brookhaven $g - 2$ Experiment,” *Phys. Rev.* **D53** (1996) 1648–1657 [[hep-ph/9507386](#)].
- [23] T. Moroi, “The Muon anomalous magnetic dipole moment in the minimal supersymmetric standard model,” *Phys. Rev.* **D53** (1996) 6565–6575 [[hep-ph/9512396](#)] [*Erratum ibid.* **D56** (1997) 4424].
- [24] B. Zhu, R. Ding, and T. Li, “Higgs mass and muon anomalous magnetic moment in the MSSM with gauge-gravity hybrid mediation,” *Phys. Rev.* **D96** (2017) 035029 [[arXiv:1610.09840](#)].
- [25] A. Choudhury, L. Darmé, L. Roszkowski, E. M. Sessolo, and S. Trojanowski, “Muon $g - 2$ and related phenomenology in constrained vector-like extensions of the MSSM,” *JHEP* **05** (2017) 072 [[arXiv:1701.08778](#)].
- [26] T. T. Yanagida and N. Yokozaki, “Muon $g - 2$ in MSSM gauge mediation revisited,” *Phys. Lett.* **B772** (2017) 409–414 [[arXiv:1704.00711](#)].
- [27] M. Endo, K. Hamaguchi, S. Iwamoto, and K. Yanagi, “Probing minimal SUSY scenarios in the light of muon $g - 2$ and dark matter,” *JHEP* **06** (2017) 031 [[arXiv:1704.05287](#)].

- [28] K. Hagiwara, K. Ma, and S. Mukhopadhyay, “Closing in on the chargino contribution to the muon $g - 2$ in the MSSM: current LHC constraints,” *Phys. Rev. D* **D97** (2018) 055035 [[arXiv:1706.09313](#)].
- [29] M. Chakraborti, A. Datta, N. Ganguly, and S. Poddar, “Multilepton signals of heavier electroweakinos at the LHC,” *JHEP* **11** (2017) 117 [[arXiv:1707.04410](#)].
- [30] A. Choudhury, S. Rao, and L. Roszkowski, “Impact of LHC data on muon $g - 2$ solutions in a vectorlike extension of the constrained MSSM,” *Phys. Rev. D* **D96** (2017) 075046 [[arXiv:1708.05675](#)].
- [31] M. A. Ajaib, “SU(5) with nonuniversal gaugino masses,” *Int. J. Mod. Phys. A* **A33** (2018) 1850032 [[arXiv:1711.02560](#)].
- [32] A. S. Belyaev, S. F. King, and P. B. Schaefers, “Muon $g-2$ and dark matter suggest nonuniversal gaugino masses: SU(5) \times A_4 case study at the LHC,” *Phys. Rev. D* **D97** (2018) 115002 [[arXiv:1801.00514](#)].
- [33] G. Bhattacharyya, T. T. Yanagida, and N. Yokozaki, “An extended gauge mediation for muon ($g - 2$) explanation,” *Phys. Lett. B* **B784** (2018) 118–121 [[arXiv:1805.01607](#)].
- [34] S. Abel, D. G. Cerdeño, and S. Robles, “The Power of Genetic Algorithms: what remains of the pMSSM?” [arXiv:1805.03615](#).
- [35] J. Cao, Y. He, L. Shang, Y. Zhang, and P. Zhu, “Current status of a natural NMSSM in light of LHC 13 TeV data and XENON-1T results,” *Phys. Rev. D* **D99** (2019) 075020 [[arXiv:1810.09143](#)].
- [36] B. Dutta and Y. Mimura, “Electron $g - 2$ with flavor violation in MSSM,” *Phys. Lett. B* **B790** (2019) 563–567 [[arXiv:1811.10209](#)].
- [37] P. Cox, C. Han, T. T. Yanagida, and N. Yokozaki, “Gaugino mediation scenarios for muon $g - 2$ and dark matter,” *JHEP* **08** (2019) 097 [[arXiv:1811.12699](#)].
- [38] H. M. Tran and H. T. Nguyen, “GUT-inspired MSSM in light of muon $g - 2$ and LHC results at $\sqrt{s} = 13$ TeV,” *Phys. Rev. D* **D99** (2019) 035040 [[arXiv:1812.11757](#)].
- [39] M. Ibe, M. Suzuki, T. T. Yanagida, and N. Yokozaki, “Muon $g - 2$ in Split-Family SUSY in light of LHC Run II,” *Eur. Phys. J. C* **C79** (2019) 688 [[arXiv:1903.12433](#)].
- [40] M. Badziak and K. Sakurai, “Explanation of electron and muon $g - 2$ anomalies in the MSSM,” *JHEP* **10** (2019) 024 [[arXiv:1908.03607](#)].
- [41] M. Abdughani, K.-I. Hikasa, L. Wu, J. M. Yang, and J. Zhao, “Testing electroweak SUSY for muon $g - 2$ and dark matter at the LHC and beyond,” *JHEP* **11** (2019) 095 [[arXiv:1909.07792](#)].
- [42] E. Kpatcha, I. Lara, D. E. López-Fogliani, C. Muñoz, and N. Nagata, “Explaining muon $g - 2$ data in the $\mu\nu$ SSM,” *Eur. Phys. J. C* **C81** (2021) 154 [[arXiv:1912.04163](#)].

- [43] T. T. Yanagida, W. Yin, and N. Yokozaki, “Muon $g - 2$ in Higgs-anomaly mediation,” *JHEP* **06** (2020) 154 [[arXiv:2001.02672](#)].
- [44] C. Han, *et al.*, “LFV and $(g-2)$ in non-universal SUSY models with light higgsinos,” *JHEP* **05** (2020) 102 [[arXiv:2003.06187](#)].
- [45] M. Chakraborti, S. Heinemeyer, and I. Saha, “Improved $(g - 2)_\mu$ Measurements and Supersymmetry,” *Eur. Phys. J.* **C80** (2020) 984 [[arXiv:2006.15157](#)].
- [46] R. Nagai and N. Yokozaki, “Lepton flavor violations in SUSY models for muon $g - 2$ with right-handed neutrinos,” *JHEP* **01** (2021) 099 [[arXiv:2007.00943](#)].
- [47] M. Chakraborti, S. Heinemeyer, and I. Saha, “Improved $(g - 2)_\mu$ Measurements and Wino/Higgsino Dark Matter.” [arXiv:2103.13403](#).
- [48] M. Endo, K. Hamaguchi, S. Iwamoto, and T. Kitahara, “Muon $g - 2$ vs LHC Run 2 in supersymmetric models,” *JHEP* **04** (2020) 165 [[arXiv:2001.11025](#)].
- [49] **ATLAS** Collaboration, “Search for direct production of electroweakinos in final states with missing transverse momentum and a Higgs boson decaying into photons in pp collisions at $\sqrt{s} = 13$ TeV with the ATLAS detector,” *JHEP* **10** (2020) 005 [[arXiv:2004.10894](#)].
- [50] **CMS** Collaboration, “Search for supersymmetry in final states with two oppositely charged same-flavor leptons and missing transverse momentum in proton-proton collisions at $\sqrt{s} = 13$ TeV.” [arXiv:2012.08600](#).
- [51] M. Endo, K. Hamaguchi, T. Kitahara, and T. Yoshinaga, “Probing Bino contribution to muon $g - 2$,” *JHEP* **11** (2013) 013 [[arXiv:1309.3065](#)].
- [52] S. Iwamoto, T. T. Yanagida, and N. Yokozaki, “Wino-Higgsino dark matter in the MSSM from the $g - 2$ anomaly.” [arXiv:2104.03223](#).
- [53] M. Muhlleitner, A. Djouadi, and Y. Mambrini, “SDECAY: A Fortran code for the decays of the supersymmetric particles in the MSSM,” *Comput. Phys. Commun.* **168** (2005) 46–70 [[hep-ph/0311167](#)].
- [54] M. M. Muhlleitner, A. Djouadi, and M. Spira, “Decays of Supersymmetric Particles — the Program SUSY-HIT,” *Acta Phys. Polon.* **B38** (2007) 635–644 [[hep-ph/0609292](#)].
- [55] P. Athron, *et al.*, “Gm2Calc: Precise MSSM Prediction for $(g - 2)$ of the Muon,” *Eur. Phys. J.* **C76** (2016) 62 [[arXiv:1510.08071](#)].
- [56] **ATLAS** Collaboration, “Search for electroweak production of charginos and sleptons decaying into final states with two leptons and missing transverse momentum in $\sqrt{s} = 13$ TeV pp collisions using the ATLAS detector,” *Eur. Phys. J.* **C 80** (2020) 123 [[arXiv:1908.08215](#)].
- [57] **ATLAS** Collaboration, “Search for direct production of electroweakinos in final states with one lepton, missing transverse momentum and a Higgs boson decaying into two b -jets in pp collisions at $\sqrt{s} = 13$ TeV with the ATLAS detector,” *Eur. Phys. J. C* **80** (2020) 691 [[arXiv:1909.09226](#)].

- [58] **CMS** Collaboration, “Search for electroweak production of charginos and neutralinos in multilepton final states in proton-proton collisions at $\sqrt{s} = 13$ TeV,” *JHEP* **03** (2018) 166 [[arXiv:1709.05406](#)].
- [59] **ATLAS** Collaboration, “Search for electroweak production of supersymmetric particles in final states with two or three leptons at $\sqrt{s} = 13$ TeV with the ATLAS detector,” *Eur. Phys. J.* **C78** (2018) 995 [[arXiv:1803.02762](#)].
- [60] M. Endo, K. Hamaguchi, S. Iwamoto, and T. Yoshinaga, “Muon $g - 2$ vs LHC in supersymmetric models,” *JHEP* **01** (2014) 123 [[arXiv:1303.4256](#)].
- [61] **ATLAS** Collaboration, “Search for chargino-neutralino pair production in final states with three leptons and missing transverse momentum in $\sqrt{s}=13$ TeV pp collisions with the ATLAS detector,” *ATLAS-CONF-2020-015*, CERN, 2020.
- [62] **CMS** Collaboration, “Search for electroweak production of charginos and neutralinos in proton-proton collisions at $\sqrt{s} = 13$ TeV,” *CMS-PAS-SUS-19-012*, CERN, 2021.
- [63] **CMS** Collaboration, “Search for chargino-neutralino production in final states with a Higgs boson and a W boson,” *CMS-PAS-SUS-20-003*, CERN, 2021.
- [64] P. von Weitershausen, M. Schafer, H. Stockinger-Kim, and D. Stockinger, “Photonic SUSY Two-Loop Corrections to the Muon Magnetic Moment,” *Phys. Rev. D* **81** (2010) 093004 [[arXiv:1003.5820](#)].
- [65] S. Marchetti, S. Mertens, U. Nierste, and D. Stockinger, “Tan(beta)-enhanced supersymmetric corrections to the anomalous magnetic moment of the muon,” *Phys. Rev. D* **79** (2009) 013010 [[arXiv:0808.1530](#)].
- [66] J. Girschbach, S. Mertens, U. Nierste, and S. Wiesenfeldt, “Lepton flavour violation in the MSSM,” *JHEP* **05** (2010) 026 [[arXiv:0910.2663](#)].
- [67] M. M. Nojiri, K. Fujii, and T. Tsukamoto, “Confronting the minimal supersymmetric standard model with the study of scalar leptons at future linear $e^+ e^-$ colliders,” *Phys. Rev. D* **54** (1996) 6756–6776 [[hep-ph/9606370](#)].
- [68] M. M. Nojiri, D. M. Pierce, and Y. Yamada, “Slepton production as a probe of the squark mass scale,” *Phys. Rev. D* **57** (1998) 1539–1552 [[hep-ph/9707244](#)].
- [69] H.-C. Cheng, J. L. Feng, and N. Polonsky, “Superoblique corrections and nondecoupling of supersymmetry breaking,” *Phys. Rev. D* **56** (1997) 6875–6884 [[hep-ph/9706438](#)].
- [70] H.-C. Cheng, J. L. Feng, and N. Polonsky, “Signatures of multi - TeV scale particles in supersymmetric theories,” *Phys. Rev. D* **57** (1998) 152–169 [[hep-ph/9706476](#)].
- [71] E. Katz, L. Randall, and S.-f. Su, “Supersymmetric partners of oblique corrections,” *Nucl. Phys. B* **536** (1998) 3–28 [[hep-ph/9801416](#)].
- [72] H. G. Fargnoli, C. Gnendiger, S. Paßehr, D. Stöckinger, and H. Stöckinger-Kim, “Non-decoupling two-loop corrections to $(g - 2)_\mu$ from fermion/sfermion loops in the MSSM,” *Phys. Lett.* **B726** (2013) 717–724 [[arXiv:1309.0980](#)].

- [73] **ATLAS** Collaboration, “Search for direct production of charginos, neutralinos and sleptons in final states with two leptons and missing transverse momentum in pp collisions at $\sqrt{s} = 8$ TeV with the ATLAS detector,” *JHEP* **05** (2014) 071 [[arXiv:1403.5294](#)].
- [74] **ATLAS** Collaboration, “Searches for electroweak production of supersymmetric particles with compressed mass spectra in $\sqrt{s} = 13$ TeV pp collisions with the ATLAS detector,” *Phys. Rev. D* **101** (2020) 052005 [[arXiv:1911.12606](#)].
- [75] LEP2 SUSY Working Group (ALEPH, DELPHI, L3, OPAL), “Combined LEP Selectron/Smuon/Stau Results, 183–208 GeV.” Notes LEPSUSYWG/04–01.1. <http://lepsusy.web.cern.ch/lepsusy/Welcome.html>.
- [76] **ATLAS** Collaboration, “Search for direct stau production in events with two hadronic τ -leptons in $\sqrt{s} = 13$ TeV pp collisions with the ATLAS detector,” *Phys. Rev. D* **101** (2020) 032009 [[arXiv:1911.06660](#)].
- [77] **CMS** Collaboration, “Search for direct pair production of supersymmetric partners to the τ lepton in proton-proton collisions at $\sqrt{s} = 13$ TeV,” *Eur. Phys. J. C* **80** (2020) 189 [[arXiv:1907.13179](#)].
- [78] LEP2 SUSY Working Group (ALEPH, DELPHI, L3, OPAL), “Combined LEP Chargino Results, up to 208 GeV for large m_0 .” Notes LEPSUSYWG/01–03.1. <http://lepsusy.web.cern.ch/lepsusy/Welcome.html>.
- [79] M. Carena, S. Gori, N. R. Shah, and C. E. M. Wagner, “A 125 GeV SM-like Higgs in the MSSM and the $\gamma\gamma$ rate,” *JHEP* **03** (2012) 014 [[arXiv:1112.3336](#)].
- [80] M. Carena, S. Gori, N. R. Shah, C. E. M. Wagner, and L.-T. Wang, “Light Stau Phenomenology and the Higgs $\gamma\gamma$ Rate,” *JHEP* **07** (2012) 175 [[arXiv:1205.5842](#)].
- [81] T. Kitahara, “Vacuum Stability Constraints on the Enhancement of the $h \rightarrow \gamma\gamma$ rate in the MSSM,” *JHEP* **11** (2012) 021 [[arXiv:1208.4792](#)].
- [82] M. Carena, S. Gori, I. Low, N. R. Shah, and C. E. M. Wagner, “Vacuum Stability and Higgs Diphoton Decays in the MSSM,” *JHEP* **02** (2013) 114 [[arXiv:1211.6136](#)].
- [83] **Particle Data Group** Collaboration, “Review of Particle Physics,” *PTEP* **2020** (2020) 083C01.
- [84] J. de Blas *et al.*, “Higgs Boson Studies at Future Particle Colliders,” *JHEP* **01** (2020) 139 [[arXiv:1905.03764](#)].
- [85] **Planck** Collaboration, “Planck 2018 results. VI. Cosmological parameters,” *Astron. Astrophys.* **641** (2020) A6 [[arXiv:1807.06209](#)].
- [86] G. Belanger, F. Boudjema, A. Pukhov, and A. Semenov, “micrOMEGAs_3: A program for calculating dark matter observables,” *Comput. Phys. Commun.* **185** (2014) 960–985 [[arXiv:1305.0237](#)].

- [87] G. Belanger, F. Boudjema, A. Pukhov, and A. Semenov, “micrOMEGAs: A Tool for dark matter studies,” *Nuovo Cim. C* **033N2** (2010) 111–116 [[arXiv:1005.4133](#)].
- [88] G. Belanger, F. Boudjema, A. Pukhov, and A. Semenov, “Dark matter direct detection rate in a generic model with micrOMEGAs 2.2,” *Comput. Phys. Commun.* **180** (2009) 747–767 [[arXiv:0803.2360](#)].
- [89] G. Belanger, F. Boudjema, A. Pukhov, and A. Semenov, “MicrOMEGAs 2.0: A Program to calculate the relic density of dark matter in a generic model,” *Comput. Phys. Commun.* **176** (2007) 367–382 [[hep-ph/0607059](#)].
- [90] LUX Collaboration, “Results from a search for dark matter in the complete LUX exposure,” *Phys. Rev. Lett.* **118** (2017) 021303 [[arXiv:1608.07648](#)].
- [91] PandaX-II Collaboration, “Dark Matter Results From 54-Ton-Day Exposure of PandaX-II Experiment,” *Phys. Rev. Lett.* **119** (2017) 181302 [[arXiv:1708.06917](#)].
- [92] XENON Collaboration, “Dark Matter Search Results from a One Ton-Year Exposure of XENON1T,” *Phys. Rev. Lett.* **121** (2018) 111302 [[arXiv:1805.12562](#)].
- [93] T. Kitahara and T. Yoshinaga, “Stau with Large Mass Difference and Enhancement of the Higgs to Diphoton Decay Rate in the MSSM,” *JHEP* **05** (2013) 035 [[arXiv:1303.0461](#)].
- [94] S. R. Coleman, “The Fate of the False Vacuum. 1. Semiclassical Theory,” *Phys. Rev. D* **15** (1977) 2929–2936. [Erratum: *Phys.Rev.D* 16, 1248 (1977)].
- [95] C. L. Wainwright, “CosmoTransitions: Computing Cosmological Phase Transition Temperatures and Bubble Profiles with Multiple Fields,” *Comput. Phys. Commun.* **183** (2012) 2006–2013 [[arXiv:1109.4189](#)].
- [96] M. Endo, K. Hamaguchi, and K. Nakaji, “Probing High Reheating Temperature Scenarios at the LHC with Long-Lived Staus,” *JHEP* **11** (2010) 004 [[arXiv:1008.2307](#)].
- [97] M. Endo, T. Moroi, M. M. Nojiri, and Y. Shoji, “Renormalization-Scale Uncertainty in the Decay Rate of False Vacuum,” *JHEP* **01** (2016) 031 [[arXiv:1511.04860](#)].
- [98] B. Batell, S. Jung, and C. E. M. Wagner, “Very Light Charginos and Higgs Decays,” *JHEP* **12** (2013) 075 [[arXiv:1309.2297](#)].
- [99] M. Endo, T. Kitahara, and T. Yoshinaga, “Future Prospects for Stau in Higgs Coupling to Di-photon,” *JHEP* **04** (2014) 139 [[arXiv:1401.3748](#)].
- [100] XENON Collaboration, “Projected WIMP sensitivity of the XENONnT dark matter experiment,” *JCAP* **11** (2020) 031 [[arXiv:2007.08796](#)].
- [101] ATLAS Collaboration, “Prospects for searches for staus, charginos and neutralinos at the high luminosity LHC with the ATLAS Detector,” *ATL–PHYS–PUB–2018–048*, CERN, 2018.

- [102] X. Cid Vidal, M. D’Onofrio, P. J. Fox, R. Torre, and K. A. Ulmer, eds., “Beyond the Standard Model physics at the HL-LHC and HE-LHC,” **CERN Yellow Reports: Monographs** **7** (2019) 585–865 [[arXiv:1812.07831](#)].
- [103] S. Gori, S. Jung, L.-T. Wang, and J. D. Wells, “Prospects for Electroweakino Discovery at a 100 TeV Hadron Collider,” **JHEP** **12** (2014) 108 [[arXiv:1410.6287](#)].
- [104] J. Bramante, *et al.*, “Relic Neutralino Surface at a 100 TeV Collider,” **Phys. Rev.** **D91** (2015) 054015 [[arXiv:1412.4789](#)].
- [105] S. Matsumoto, S. Shirai, and M. Takeuchi, “Indirect Probe of Electroweakly Interacting Particles at the High-Luminosity Large Hadron Collider,” **JHEP** **06** (2018) 049 [[arXiv:1711.05449](#)].
- [106] S. Matsumoto, S. Shirai, and M. Takeuchi, “Indirect Probe of Electroweak-Interacting Particles with Mono-Lepton Signatures at Hadron Colliders,” **JHEP** **03** (2019) 076 [[arXiv:1810.12234](#)].
- [107] S. Chigusa, Y. Ema, and T. Moroi, “Probing electroweakly interacting massive particles with Drell–Yan process at 100 TeV hadron colliders,” **Phys. Lett.** **B789** (2019) 106–113 [[arXiv:1810.07349](#)].
- [108] T. Abe, S. Chigusa, Y. Ema, and T. Moroi, “Indirect studies of electroweakly interacting particles at 100 TeV hadron colliders,” **Phys. Rev.** **D100** (2019) 055018 [[arXiv:1904.11162](#)].
- [109] M. Endo, K. Hamaguchi, S. Iwamoto, T. Kitahara, and T. Moroi, “Reconstructing Supersymmetric Contribution to Muon Anomalous Magnetic Dipole Moment at ILC,” **Phys. Lett. B** **728** (2014) 274–281 [[arXiv:1310.4496](#)].
- [110] L. Beresford and J. Liu, “Search Strategy for Sleptons and Dark Matter Using the LHC as a Photon Collider,” **Phys. Rev. Lett.** **123** (2019) 141801 [[arXiv:1811.06465](#)].